On the Determination of the Diffusion Coefficients of Electrons and of Potassium Ions in Copper(II) Hexacyanoferrate(II) Composite Electrodes

H. Kahlert, U. Retter,† H. Lohse,† K. Siegler,† and F. Scholz*

Institut für Chemie, Humboldt-Universität zu Berlin, Hessische Strasse 1-2, D-10115 Berlin, Germany

Received: March 25, 1998; In Final Form: July 26, 1998

Composite electrodes of graphite, paraffin, and copper(II) hexacyanoferrate(II) (Cu hcf) were studied by cyclic voltammetry (0.05−1000 mV s^{-1}) and electrochemical impedance spectroscopy (10 Hz to 1 MHz). Cyclic voltammetric measurements were also performed with copper(II) hexacyanoferrate(II) which was mechanically immobilized on a paraffin impregnated graphite electrode (PIGE). The Nyquist plots which were obtained from impedance measurements could be modeled with an adsorption process in series to the charge transfer of K^+ ions between the electrolyte solution and the Cu hcf, the diffusion of K^+ ions in the Cu hcf, and the conduction of electrons in the Cu hcf. The charge transfer and the diffusion of K^+ ions obeys the Randles mechanism. The charge transfer resistance as well as the Warburg coefficient exhibit a minimum at the formal potential. Both effects could be explained theoretically on the basis of the potential dependence of the oxidized and reduced forms of Cu hcf. The electron transfer from the graphite to the Cu hcf is so fast that even at 1 MHz it was impossible to determine its rate constant. The conduction of electrons in the Cu hcf exhibits the feature of a diffusion process with a transmissive boundary. The experiments proved that a surface oxidation of the graphite has no influence on the electrode kinetics. However, for the first time it has been possible to separately determine the diffusion coefficients of ions and electrons by impedance spectroscopy. With other techniques, e.g., cyclic voltammetry only an effective diffusion coefficient for a coupled transport of cations and electrons is accessible. With cyclic voltammetry a diffusion coefficient of K^+ ions ((1.49 ± 0.04) × 10^{-9} cm^2 s^{-1}) and a rate constant of ion transfer ((1.42 ± 0.05) × 10^{-7} m s^{-1}) were determined. Impedance spectroscopy at low frequencies yields the same diffusion coefficient for K^+ ions ((1.4 ± 0.2) × 10^{-9} cm^2 s^{-1}). The rate constant for potassium ion transfer between the electrolyte solution and the Cu hcf was found to be (3.0 ± 0.2) × 10^{-6} m s^{-1}. In the high-frequency range it was possible to determine the diffusion coefficient of electrons as (0.10 ± 0.01) cm^2 s^{-1}. In the case of mechanically immobilized particles, the rate constant for the ion transfer was determined with the help of cyclic voltammetry as (2.0 ± 0.2) × 10^{-7} m s^{-1}.

Introduction

Reactive electrodes (reactrodes) made of graphite, paraffin, and an ion-selective material offer interesting new possibilities as ion-selective electrodes.[1−4] Solid metal hexacyanometalates of the type $(M^+)_nM'[M''(CN)_6]$, where M′ and M″ denote transition metals, are very useful as ion-selective materials, because the redox reaction of lattice metal ions are accompanied by a reversible exchange of cations between the electrolyte solution and interstitial holes of the solid compound (see the cubic structure depicted in Figure 1). Several ion selective electrodes based on thin films of these compounds have been developed.[5−9] From a technical point of view, it is attractive to use these materials in compact reactrodes.[2−4] For the investigation of such modified electrodes, cyclic voltammetry, and other electrochemical techniques involving large perturbations have been used. However, the electrochemical impedance spectroscopy offers several advantages for studying such complex systems.[6,10] These are the wide frequency range, which allows a convenient determination of kinetic as well as mass-transport parameters, and the low perturbation from equilibrium by the low-amplitude sinusoidal voltage.

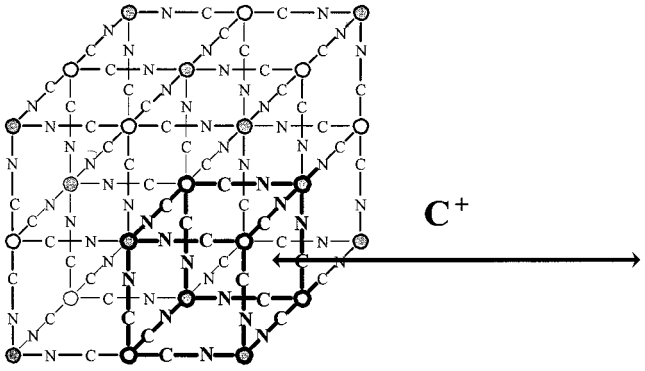

Figure 1. Schematic description of the structure of copper(II) hexacyanoferrate(II). The iron(II) ions (○) are linked to the carbon of the cyanide ions, whereas the copper(II) ions (●) are linked to the nitrogen atoms.

In this paper, cyclic voltammetric, chronocoulometric and impedance measurements with copper(II) hexacyanoferrate(II) in composite electrodes in KNO_3 solution are presented. For comparison, data from cyclic voltammetric and impedance measurements for copper(II) hexacyanoferrate(II) mechanically

* To whom correspondence should be addressed. Tel.: +49(030)2093-7518. Fax: +49(030)2093-6985. E-mail: fritz=scholz@chemie.hu-berlin.de.

† BAM Berlin, Rudower Chaussee 5, D-12489 Berlin, Germany.

10.1021/jp981623q CCC: $15.00
Published on Web 10/13/1998

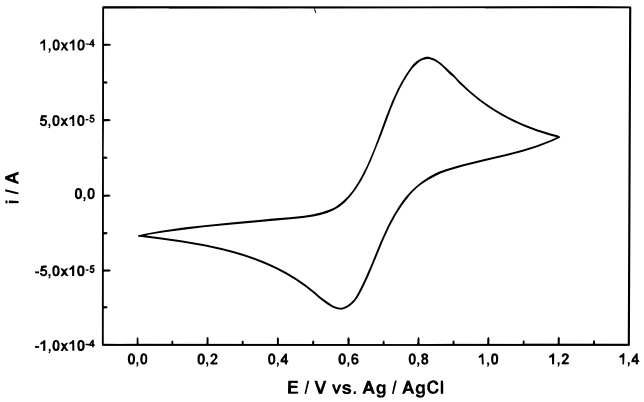

Figure 2. Typical cyclic voltammogram of a Cu hcf composite electrode (Cu2.5-un). The electrolyte solution contained 0.1 mol l^{-1} KNO_3. The scan rate was 50 mV s^{-1}. The starting potential was 1.2 V vs Ag/AgCl.

attached to a paraffin impregnated graphite electrode (PIGE) are also presented. During oxidation/reduction reactions electrons are exchanged between the graphite surface and the particles in the bulk of the electrode, whereas potassium ions are exchanged between the particles and the adjacent electrolyte. The net reaction is given by the following equation (The subscript s denotes solid phases.):

$$\underset{\text{oxidized form}}{\{KCu[Fe^{3+}(CN)_6]\}_s} + K^+ + e^- \rightleftarrows \underset{\text{reduced form}}{\{K_2Cu[Fe^{2+}(CN)_6]\}_s} \quad (1)$$

Figure 2 shows a typical cyclic voltammogram for a Cu hcf composite electrode immersed in 0.1 mol l^{-1} KNO_3 as an electrolyte solution. In the entire accessible potential range, going to almost −2 V vs Ag/AgCl, the copper ions in the Cu hcf are not reducible to copper(I) or copper(0).

In several previous publications on the electrochemistry of metal hexacyanoferrates, an effective diffusion coefficient for the coupled electron/ion transport has been reported.[6,11,12] It was only Murray et al. who attempted to determine a diffusion coefficient for electrons in Prussian blue.[13−15] They used pulse techniques and interdigitated array electrodes for so-called "time-of-flight" experiments. They assumed the obtained diffusion coefficients to be those of electrons, although they were of the same order of magnitude as the diffusion coefficients of cations. From our findings it can be inferred that Murray indeed determined only the effective diffusion coefficient of ion/electron transport, which is basically the diffusion coefficients of cations. The diffusion coefficients of electrons are only accessible in a much higher frequency domain, i.e., in the MHz range.

The model Description of the Electrode. The copper(II) hexacyanoferrate(II) consists of agglomerates of microcrystals (cf. the transmission electron micrograph given in Figure 3). Figure 4a describes schematically the situation for copper hexacyanoferrate particles mechanically attached to a PIGE. The particle is in contact with a more or less plane surface of a graphite electrode. Figure 4b depicts the situation for a composite electrode. Such composite electrodes consist of large graphite particles (around 150 μm), smaller hexacyanoferrate particles (around 30 μm), and paraffin. The hexacyanoferrate particles are embedded in the paraffin−graphite matrix. Some of the particles have a contact area to the electrolyte solution and to graphite particles and so they can be electrochemically active. Hexacyanoferrate particles in the bulk of the electrode rod which have neither contact with the electrolyte solution nor with the graphite particles are electrochemically inactive

Figure 3. Transmission electron micrographs of Cu hcf particles.

because, during oxidation and reduction, both the electrons and cations must be exchanged.

The surface of graphite may be covered by numerous functional groups, such as phenol, carbonyl, carboxyl, quinone, lactone, and peroxide groups.[16] These groups form an oxidized film at the electrode surface which can be obtained either by chemical[16] or electrochemical[17−20] oxidation. The presence of these functional groups can decrease the overvoltage for the hydrogen evolution and, in this way, impair the working window of the carbon electrode.[21] On the other hand, these surface groups can very effectively catalyze several redox reactions which are otherwise strongly inhibited at bare carbon electrodes.[19,22,23] To characterize electrode surfaces, very often hexacyanoferrate anions have been used as the determined charge transfer rates allow to draw conclusions on their catalytic activity. However, in several solution studies it has been shown that the oxidation state of graphite electrodes does not significantly influence the charge-transfer rate of the dissolved hexacyanoferrate system. The oxidation state of graphite surfaces is much better monitored by the charge-transfer rate of, e.g., NADH oxidation.[16] Engel et al. performed impedance measurements on glassy carbon electrodes covered with thin films of Cu hcf. The differences in charge-transfer resistance which he has obtained, have been assigned to different pretreatments of the glassy carbon substrate.[5,11] It should already be remarked at this point that Engel et al., according to our results, indeed determined the charge transfer rate for the potassium ions. These authors measured the impedance only up to 100 kHz. To test the hypothesis of Engels et al. that the surface properties of the carbon electrode have an important influence on the kinetics of the electrode reaction, two types of graphite, one with an oxidized surface and one without a deliberately oxidized surface, were used.

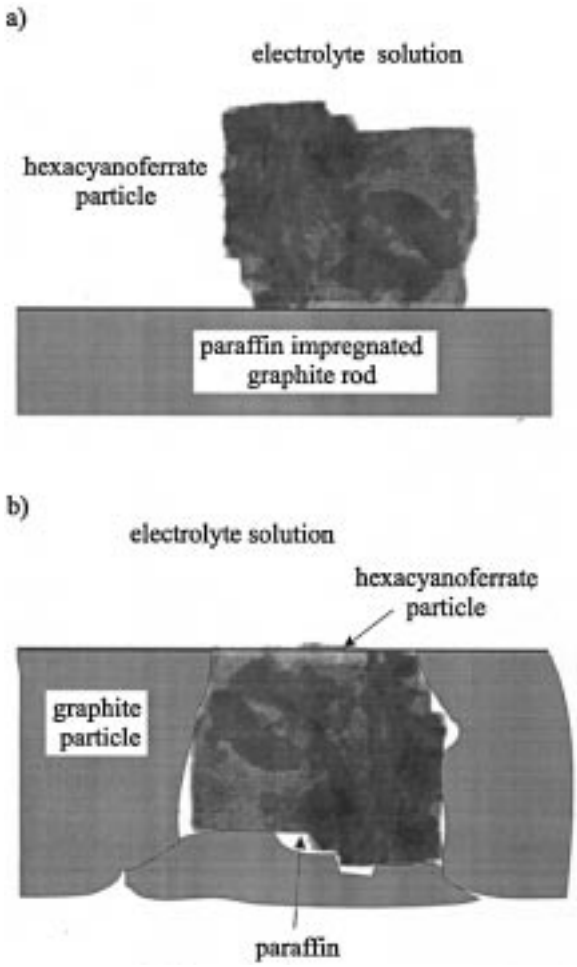

Figure 4. (a) Schematic illustration of a Cu hcf particle mechanically attached to a PIGE. (b) Schematic illustration of a part of the surface of a composite electrode with a Cu hcf particle, which is embedded in the graphite−paraffin matrix and has interfaces with the electrolyte solution and with graphite particles.

Experimental Section

Equipment. Chonocoulometry and cyclic voltammetry (CV) were performed using an AUTOLAB system with a PGSTAT 20 (Eco-Chemie, Utrecht, Netherlands) in conjunction with a three-electrode system and a personal computer (IBM compatible). The reference electrode was an Ag/AgCl electrode (3 M KCl) (Metrohm, Herisau, Switzerland) with a potential of 0.208 V vs SHE at 25 °C. A platinum wire served as an auxiliary electrode. With exception of the case of impedance measurements, the solutions were *not* purged with nitrogen because, in the potential range of the activity of Cu hcf, there is no interference by oxygen.

Electrochemical impedance spectroscopy (EIS) was performed with an LF impedance analyzer 41921A (Hewlett-Packard) in conjunction with a personal computer (IBM compatible) for data acquisition and treatment. With this equipment, impedance spectra are accessible in a frequency range from 5 Hz to 13 MHz; however, in this study the highest frequency used was 1 MHz. At each frequency 20 single measurements were made and automatically averaged. The instrument for the impedance measurements was connected to a two electrode cell with a platinum sheet as the auxiliary electrode, bent in a way as to be situated in front of the working electrode surface. The latter was the composite electrode. The typically applied low-amplitude sinusoidal voltage was 10 mV. Each measurement was performed at a potential which was adjusted by a dc voltage between the two electrodes monitored by measurement versus a reference electrode (Ag/AgCl as given above) with the help of a high input resistance voltmeter (MV 88, Praecitronic, Germany). The measurements were performed at 10 mV increments in a potential range from 640 to 740 mV vs Ag/AgCl, which is just around the formal potential of the hexacyanoferrate system of the solid Cu hcf.

Chemicals. Copper(II) hexacyanoferrate(II) (Cu hcf) was synthesized by dropwise addition of a solution of 0.82 g of $CuCl_2 \cdot 4H_2O$ in 50 mL of bidistilled water to a solution of 2 g of $K_4[Fe(CN)_6]$ in 30 mL of bidistilled water. The reddish brown precipitate was washed with water and dried under vacuum at ambient temperature. From transmission electron micrographs (taken at the Institute of Inorganic Chemistry of the Czech Academy of Sciences, Rez, Czechoslavakia) and from particle size analysis with a Laser Partikel Analysator 3.400 (Grimm Labortechnik GmbH, Ainring, Germany), the average size of the Cu hcf agglomerates of 30 μm was determined.

The oxidation of the surface of commercial graphite powder was achieved by reflux boiling of the graphite powder with concentrated nitric acid in a weight ratio 1:10 for 4 h. Following the cooling of the mixture, the graphite was filtered and washed with water until tests of the water washing revealed a neutral pH. Then the graphite powder was dried. It has been observed previously[1] that this procedure leads to a graphite with an oxidized surface which strongly catalyses the electrochemical reaction of quinhydrone.

All the following chemicals used throughout this study were of p.a. quality: KNO_3, $K_2[Fe(CN)_6]$, $CuCl_2 \cdot 4H_2O$ (VEB Laborchemie Appolda, Germany), graphite powder (VEB GERMED Dresden, Germany), paraffin mp 56−58 °C (VEB HB Labor und Feinchemikalien, Sebnitz, Germany), nitric acid (65%) (Merck-Schuchardt, Germany).

Electrode Preparation. *(i) Composite Electrodes.* Graphite powder (0.95 g) and 0.05 g of copper hexacyanoferrate (Cu hcf) were thoroughly mixed in an agate mortar for at least 10 min. This powder was added to 1 g of solid paraffin, and the mixture was heated to melt the paraffin. The liquid paste was again thoroughly mixed before it was pressed into polyethylene tubes (length, 4 cm; inner diameter, 5 mm). After solidification, the tube was removed and the electrode rod was insulated with melted paraffin. This insulation was removed at one end of the electrode rod for making the electrical connection to the potentiostat. It was also removed at the other end to give a reproducible circular electrode surface after polishing. Before each measurement the electrode surface could be polished on white printing paper. The total geometric surface area was $A = 0.196$ cm^2.

The studied electrodes were designated as follows: the electrode with untreated graphite, Cu2.5-un; and the electrode with oxidized graphite, Cu2.5-ox. (The number 2.5 refers to the percent content of Cu hcf in the electrodes.)

(ii) Particles Mechanically Attached to a Paraffin Impregnated Graphite Electrode (PIGE). Paraffin-impregnated graphite electrodes (PIGEs) with a diameter of 5 mm were used. The preparation of the impregnated graphite rods as well as the immobilization of solid particles on the electrode surface have been described elsewhere.[24,25] The graphite rods were those for spectral analysis (VEB Elektrokohle, Germany).

Results and Discussion

1. Chronocoulometric Measurements. Chronocoulometric measurements were performed to determine the active surface area, the active volume, and the concentrations of oxidized and

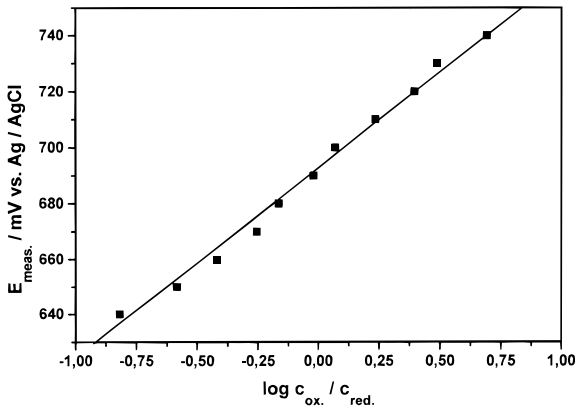

Figure 5. Plot of the electrode potential versus the logarithm of the ratio c_{ox}/c_{red} for the Cu2.5-un composite electrode. The electrolyte solution contained 0.1 mol l^{-1} KNO_3.

reduced centers at a certain potential of the Cu2.5-un and Cu2.5-ox electrodes. These data are necessary for the estimation of the diffusion coefficient and the reaction rate by CV and EIS measurements. Multistep chonocoulometry was used in the following way: To determine the concentration of oxidized iron centers at a certain potential, the electrode was first polarized during 400 s at 0 V to reduce all active centers. Then, the charge for oxidation was measured within the following 400 s at set potentials between 640 and 740 mV with a 10 mV spacing. To determine the concentration of reduced iron centers, the electrode was first polarized during 400 s at 1.2 V to oxidize all active centers. Then the charge for reduction was measured within the following 400 s at a set potential between 740 and 640 mV with a 10 mV spacing. From the maximum electric charge Q the total number n_{total} of redox centers was calculated to be $(4.78 \pm 0.08) \times 10^{-8}$ mol. To obtain the concentrations of oxidized and reduced centers at a certain potential it was necessary to estimate the volume over which these active centers are distributed. The total concentration of iron centers in the Cu hcf lattice can be calculated with the help of the lattice constant (1 nm) and the number of iron centers per unit cell, which is 4 according to the stoichiometry of the compound. This total concentration is $c_{total} = 6.64 \times 10^{-3}$ mol cm^{-3}. From the simple equation for the concentration $c_{total} = n_{total}/V_{ac}$, the active volume can be determined as $V_{ac} = (7.2 \pm 0.1) \times 10^{-6}$ cm^3. This active volume can be calculated as $V_{ac} = A_{ac}d$, where A_{ac} denotes the active area and d denotes the penetration depth. The penetration depth d was taken as equal to the average size of Cu hcf particles, i.e., 30 μm. Hence, it follows that the active area is $(2.40 \pm 0.03) \times 10^{-3}$ cm^2. This value is smaller than expected and based on a simple geometric estimate of the active surface area of a composite electrode with a total surface area of $A = 0.196$ cm^2. If the Cu hcf which is incorporated in the composite electrode would expose its surface according to its content, this would give a surface area of about 4.9×10^{-3} cm^2 for the Cu2.5 electrodes. The reasons for the discrepancy between the experimental active surface area and the geometric surface area of the Cu hcf are (i) a possible coverage of some of the Cu hcf particles by a paraffin film, and (ii) not all particles can be active because some of them either lack the contact to graphite or to the electrolyte solution. Figure 5 depicts a plot of the electrode potential versus the logarithm of the ratio c_{ox}/c_{red}. This plot has a slope of 70.5 mV and gives a formal potential of 692.4 mV. As expected, both the Cu2.5-un and the Cu2.5-ox electrodes exhibited no significant differences in respect to the determined concentrations.

2. Cyclic Voltammetry. From cyclic voltammetry at different scan rates the diffusion coefficient of potassium ions and the reaction rate for the net reaction (1) can be obtained. For a reversible reaction and semiinfinite planar diffusion the peak separation ΔE_p should be 60 mV (for $z = 1$ and $T = 298$ K). In the case of the two composite electrodes, the peak separation decreases to about 30 mV at a scan rate of 0.05 mV s^{-1}. Between 0.05 and 10 mV s^{-1} the peak current depends linearly on the scan rate which bears witness of the fact that the entire amount of accessible Cu hcf at the electrode surface is electrochemically converted. At scan rates around 0.1 mV s^{-1} the peak separation increased to 60 mV. When scan rates higher than 20 mVs^{-1} are used, the peak separation increases and the peak current depends linearly on the square root of the scan rate. From theory one expects for a reversible reaction as (1) under semiinfinite planar diffusion condition that the peak current will depend on the square root of scan rate according to the relationship:

$$i_p = 2.69 \times 10^5 z^{3/2} A D^{1/2} c_{total}\, \upsilon^{1/2} \qquad (2)$$

From the slope $B = 16.55 \times 10^{-5}$ mol $s^{-1/2}$ of the linear dependence of peak current on the square root of the scan rate the diffusion coefficient can be determined as follows:

$$D = \left(\frac{B}{2.69 \times 10^5\, z^{3/2}\, Ac_{total}} \right)^2 \qquad (3)$$

This procedure gives a diffusion coefficient of $(1.49 \pm 0.04) \times 10^{-9}$ cm^2 s^{-1} for the Cu2.5-un and Cu2.5-ox electrodes. For this measurement the scan rate range was chosen from 20 up to 1000 mVs^{-1}. The obtained diffusion coefficient is in the same order of magnitude as those determined by other authors[5,6,11,12] (see also Table 1). The good agreement between these data supports the validity of our model.

The increasing peak separation, which is typical for a quasi-reversible system, and which is observed in the range from 0.1 up to 1000 mV s^{-1} is indicative for either (i) a slow electron transfer between the graphite and the Cu hcf, (ii) a slow electron transfer from one redox center to the other inside the Cu hcf particles (small electron hopping rate), or (iii) a slow transfer of cations K^+ between the solution and the Cu hcf. The square root dependence of peak currents on scan rate indicates that, under these conditions, the electrode reaction propagates only to a certain depth into the particles due to a diffusion process. For a quasi-reversible process a dependence of the peak currents

TABLE 1: Comparison of the Obtained Kinetic Parameters with Those Found by Other Authors

author	method	diffusion coefficient of electrons D_e/cm^2 s^{-1}	diffusion coefficient of K^+ D_K/cm^2 s^{-1}	rate constant of ion transport k_S/m s^{-1}
Kuwana et al. [6, 12]	CV			2.2×10^{-7}
	EIS			1.1×10^{-8}
Engel [5, 11]	CV		3.5×10^{-9}	1.3×10^{-7}
	EIS			4.5×10^{-7}
present study	CV	0.10 ± 0.01	$(1.49 \pm 0.04) \times 10^{-9}$	$(1.42 \pm 0.05) \times 10^{-7}$
	EIS		$(1.4 \pm 0.2) \times 10^{-9}$	$(3.0 \pm 0.2) \times 10^{-6}$

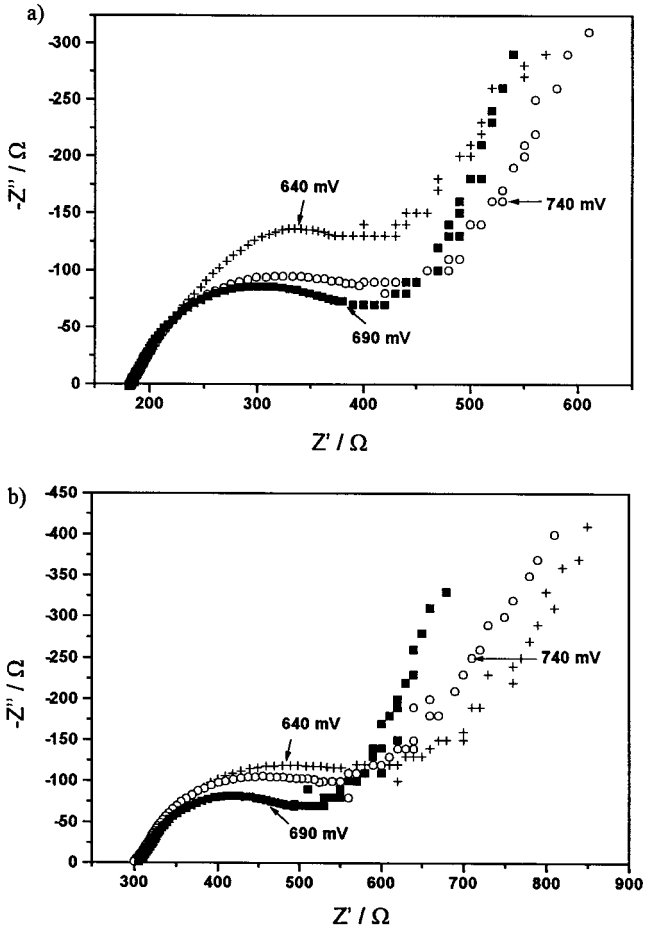

Figure 6. (a) Experimental Nyquist plots of the Cu2.5-un composite electrode impedance in a frequency range from 10 Hz to 1 MHz for 640 mV (+), 690 mV (■) and 740 mV (○) vs Ag/AgCl. The electrolyte solution contained 0.1 mol l^{-1} KNO_3. (b) experimental Nyquist plots of the Cu2.5-ox composite electrode impedance in a frequency range from 10 Hz to 1 MHz for 640 mV (+), 690 mV (■), and 740 mV (○) vs Ag/AgCl. The electrolyte solution contained 0.1 mol l^{-1} KNO_3.

on the square-root of scan rate would be unexpected. The fact that this dependence is obeyed in our case despite the obvious quasi-reversibility might be attributed to a relatively small influence of the rate constant on peak currents or also to deviations of the diffusion regime from the assumed planarity.

Cyclic voltammetry alone does not allow any decision on whether it is the electron or cation transfer which is rate determining.

In the range from 0.1 up to 20 mV s^{-1} almost the same rate constants have been obtained by applying the Nicholson−Shain formalism.[26] For the Cu2.5-un and Cu2.5-ox electrodes, a value for k_S of (1.42 ± 0.05) m s^{-1} and in the case of PIGE a value of (2.0 ± 0.2) × 10^{-7} m s^{-1} were determined. In the latter case the same diffusion coefficient was used as for the composite electrodes. These rate constants are also of the same order of magnitude as those determined by other authors (see Table 1).

3. Electrochemical Impedance Spectroscopy. For both the Cu2.5-un and the Cu2.5-ox electrodes, characteristic Nyquist plots were obtained in a frequency range from 10 Hz to 1 MHz and for several potentials (see Figure 6a and b). A first trial to model the experimental Nyquist plots on the basis of a simple Randles equivalent circuit in series to an adsorption process, used by several other authors for solid hexacyanoferrates,[6,10,11] did not give a satisfactory agreement. The very small total amounts of active Cu hcf at our electrodes, and certainly also

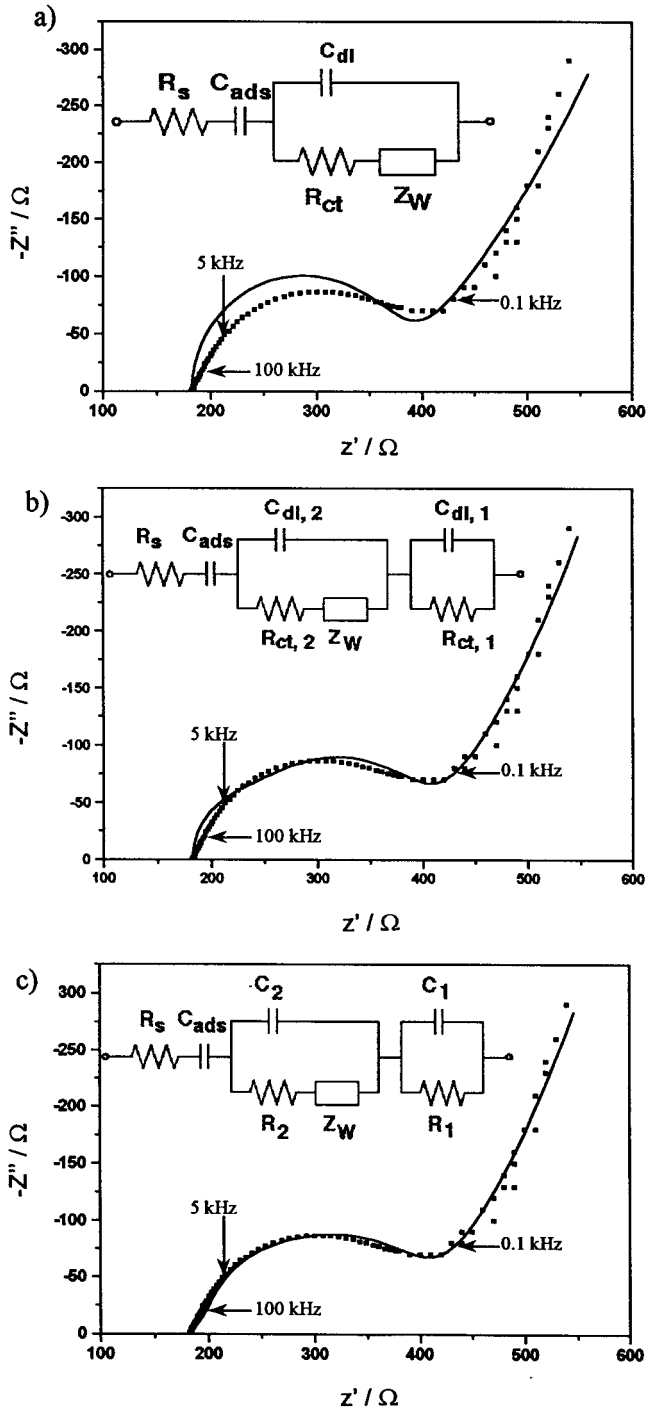

Figure 7. Experimental Nyquist plots of the Cu2.5-un composite electrode impedance in a frequency range from 10 Hz to 1 MHz at 690 mV vs Ag/AgCl (■) and Nyquist plots (full line) modeled with the depicted equivalent circuits. R_s is the resistance of the electrolyte solution; C_{ads} is the adsorption capacity. Charge-transfer processes are characterized by the double layer capacity C_{dl} and the charge-transfer resistance R_{ct}. Z_w is the Warburg impedance. The diffusion with a transmissive boundary is described by the capacity C_1 and the resistance R_1. The electrolyte solution contained 0.1 mol l^{-1} KNO_3.

the expanded frequency range allowed a much more detailed modeling. The shape of the Nyquist plots was such that a second semicircle could be assumed to be present in the high-frequency range. Therefore a model with an additional charge-transfer process was considered next. Although this model better agreed with the experiments, it soon became clear that it had to be refined by assuming a diffusion with a transmissive boundary for the high-frequency process. Figure 7 depicts the

experimental and modeled Nyquist plots together with the three described equivalent circuits. From this figure it is obvious that the third model gives by far the best agreement. The most probable interpretation of the equivalent circuit is as follows: In the high-frequency range (roughly between 50 kHz and 1 MHz), the diffusion of electrons can be described by the parallel combination of the resistance R_1 and the capacity C_1 assuming a finite diffusion space with a transmissive boundary. At medium frequencies (roughly between 400 Hz and 50 kHz), the charge transfer of potassium ions between the solution and the solid Cu hcf can be described by a simple Randles circuit with the charge-transfer resistance $R_{ct,2}$, the double layer capacity $C_{dl,2}$, and a Warburg impedance Z_{W2}. The frequency dependence of the Warburg impedance for semiinfinite planar diffusion can be described by

$$Z_{W2} = (\omega)^{1/2}\,\sigma\,(1 - j) \tag{4}$$

Here, σ is defined as the Warburg coefficient. ω is defined as the angular frequency $2\pi f$, with f being the measuring frequency.

The adsorption capacity is probably to be ascribed to the adsorption of potassium ions at the solution−Cu hcf interface.

The modeling of the finite diffusion of the electrons was performed following the work of Macdonald,[27] Buck et al.,[28] and Albery et al..[29] These authors describe a diffusion of electrons in a finite space. At very high frequencies the electrons will not be able to reach the spatial boundary and this will lead to a straight line with a 45° slope in the Nyquist plot. At slightly lower frequencies, the electrons may reach the spatial boundary. If this is an interface which is not permeable for electrons and which therefore would act as a reflecting interface, one expects in the Nyquist plot a vertical line because the impedance is solely determined by the capacity with a constant resistance. When the spatial boundary is an interface with a permeability for electrons, i.e., if it is a so-called transmissive boundary, one expects that the Nyquist plot passes from a straight line with 45° slope at high frequencies to a semicircle at slightly lower frequencies. The semicircle is due to the parallel combination of C_1 and R_1. C_1 and R_1 are both proportional to l_e, the thickness of the finite-length region, i.e.,[27]

$$3C_1R_1 = l_e^2/D_e = r \tag{5}$$

with D_e the diffusion coefficient of the electrons. Interestingly, C_1 is proportional to l_e and not to l_e^{-1} as in an ordinary plane parallel capacity. The generalized Warburg impedance Z_{W1} for semiinfinite planar diffusion in a finite-length region with transmissive boundary is[27]

$$Z_{W1} = (R_1/(j\omega r)^{1/2})\tanh((j\omega r)^{1/2}) \tag{6}$$

The real and the imaginary part of Z_{W1} have been derived in the paper of P. Drossbach et al.[30] (their k corresponds to our R_1):

$$Z_{W1} = (R_1(2\omega r)^{-1/2}/(ch((2\omega r)^{-1/2}) + \cos((2\omega r)^{-1/2})))\,(sh\,((2\omega r)^{1/2}) + \sin((2\omega r)^{1/2}) - j(sh((2\omega r)^{1/2}) - \sin((2\omega r)^{1/2}))) \tag{7}$$

Indeed, for a diffusion length $l_D = (D/\omega)^{-1/2} \ll l_e$, Z_{W1} approaches $Z_{w1\infty}$ which shows a straight line with a 45°-slope:

$$Z_{W1\infty} = (D_e/2\omega)^{1/2}\,(R_1/l_e)\,(1 - j) \tag{8}$$

The experimental data bear witness that this is an appropriate model for the Cu hcf system in composite electrodes. In Figure 4b the situation at the surface of the composite electrode is given. From this it is easily understandable that the electrode reaction can start at the three-phase boundary which is formed by the graphite, the Cu hcf, and the electrolyte solution. Only at that boundary the transfer of electrons and cations can take place in a charge compensating way. The reaction will proceed with a planar front through the microcrystals.[31] The experimental Nyquist plots prove that the diffusion of the cations indeed proceeds according to a planar diffusion regime. The diffusion of electrons which is detectable in the highest accessible frequency range, also follows a planar diffusion regime. Due to the embedding of the crystals into the graphite-paraffin matrix, this planar diffusion front of the electrons can reach the graphite interface at slightly lower frequencies. This graphite interface forms the transmissive boundary as described above.

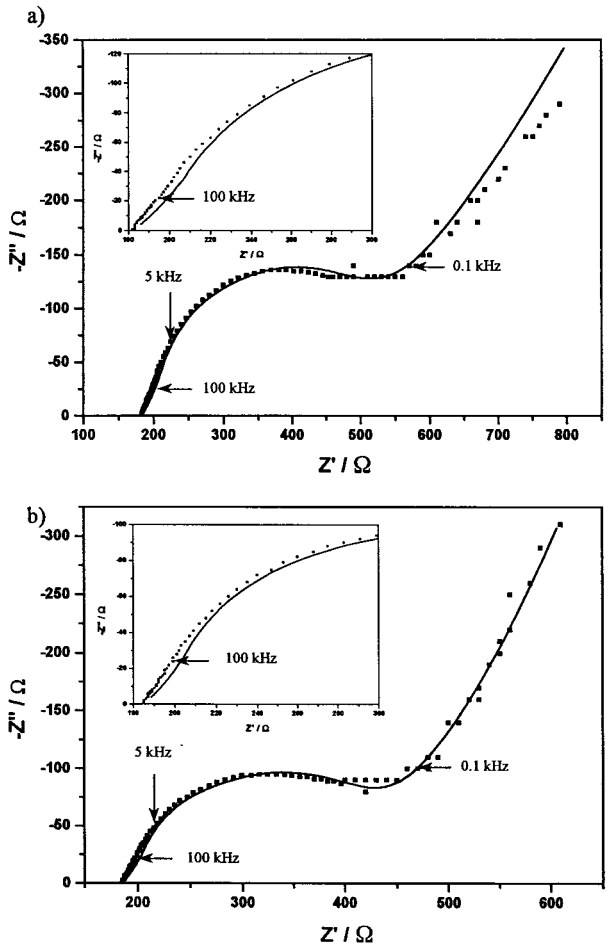

Figure 8. (a) Experimental Nyquist plot of the Cu2.5-un composite electrode in a frequency range from 10 Hz to 1 MHz at 640 mV vs Ag/AgCl (■) and Nyquist plot (full line) modeled with the equivalent circuit described in Figure 7c. (b) Experimental Nyquist plot of the Cu2.5-un composite electrode in a frequency range from 10 Hz to 1 MHz at 740 mV vs Ag/AgCl (■) and Nyquist plot (full line) modeled with the equivalent circuit described in Figure 7c.

The good agreement of the model with experimental data holds not only for the formal potential of the electrode but also in the whole potential range which was used in this study as it should be demonstrated in Figure 8a and b. Figure 9 shows that there is no frequency dispersion as in the entire range a very good agreement is observed between the experimental and modeled data. The reliability of the model and the parameters R_1, C_1, $R_{ct,2}$, $C_{dl,2}$, σ, and C_{ads} is strongly supported by the results

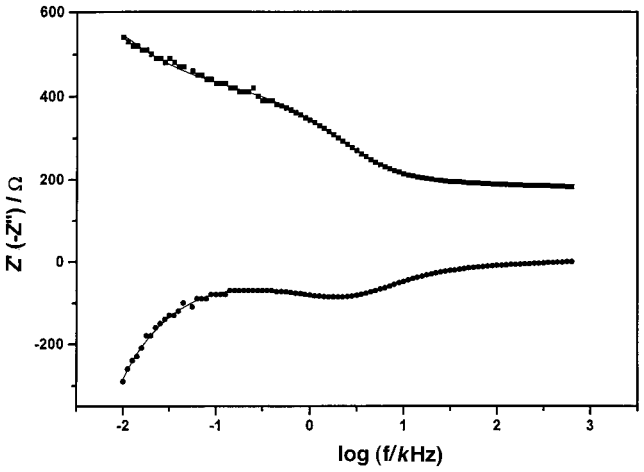

Figure 9. Plot of Z' (experimental values) and Z'' (experimental values) versus logarithm of the frequency. The full line represents the modeled data.

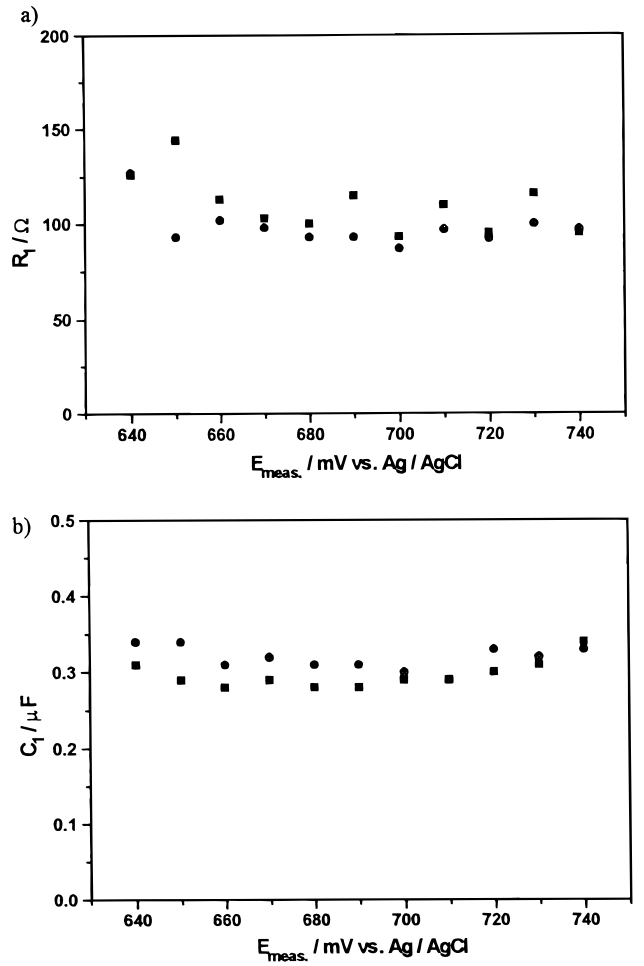

Figure 10. (a) Plot of R_1 versus the electrode potential for the Cu2.5-un (●) and the Cu2.5-ox (■) composite electrodes. (b) Plot of C_1 versus the electrode potential for the Cu2.5-un (●) and the Cu2.5-ox (■) composite electrodes.

of the nonlinear regression analysis (Marquardt). For all Nyquist impedance plots modeled, the percentage standard error of the parameters was less than 20% and the relative mean deviation between experimental and theoretical impedance values did not exceed 10%.

In the following, a detailed discussion of the parameters determined above will be given: the resistance R_1 has the same

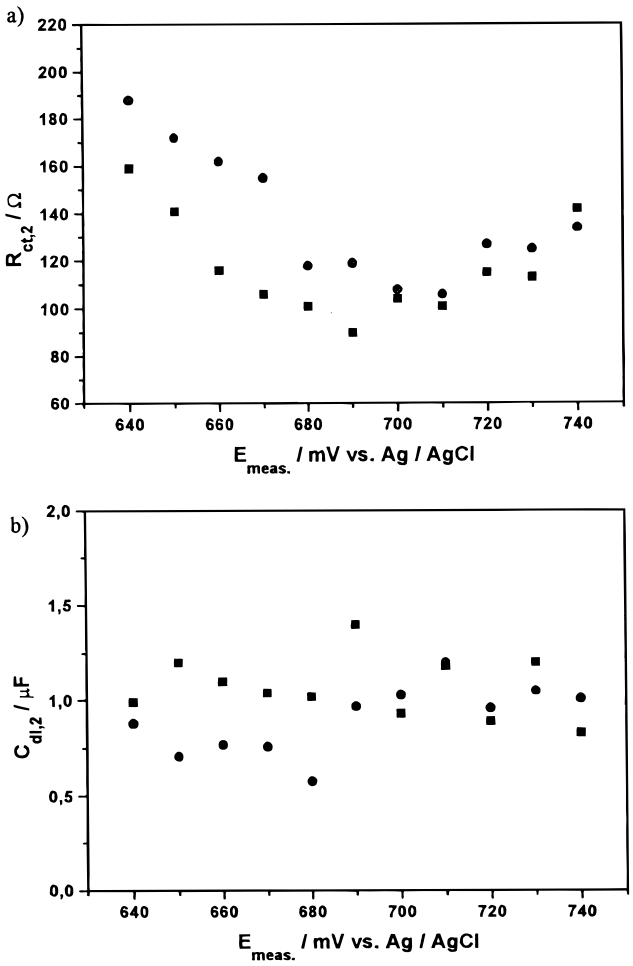

Figure 11. (a) Plot of $R_{ct,2}$ versus the electrode potential for the Cu2.5-un (●) and the Cu2.5-ox (■) composite electrodes. (b) Plot of $C_{dl,2}$ versus the electrode potential for the Cu2.5-un (●) and the Cu2.5-ox (■) composite electrodes.

value for both composite electrodes and is practically independent of the potential (see Figure 10a). It is a bulk parameter for the diffusion of the electrons through the copper hexacyanoferrate and so it is expected to be independent of the type of graphite. The specific resistance ρ can be obtained from R_1 according to $\rho = R_1A/d = (82 \pm 6)\ \Omega$ cm. The fact that this resistance is independent of the potential suggests that the electron transport cannot be described as a hopping mechanism, because this would lead to a dependence of the rate on the ratio of oxidized to reduced centers. However, the lack of potential dependence of the diffusion coefficient is consistent with a conduction mechanism as it is known for semiconducting materials based on a band model. This observation was also made in case of the three redox states of Prussian Blue.[32] The capacity C_1 is also independent of both the type of graphite and the applied potential and it has a value of (0.128 ± 0.004) mF cm^{-2} (see Figure 10b). From eq 5 and with $l_e = d$ (the size of a Cu hcf particle), it follows that the diffusion coefficient for electrons in copper hexacyanoferrate could be calculated according to

$$D_e = \frac{d^2}{C_1 R_1 3} \tag{9}$$

This results in a value of $D_e = (0.10 \pm 0.01)$ cm^2 s^{-1}. This value is very large compared to all other diffusion coefficients, which additionally supports the idea of a conduction via a

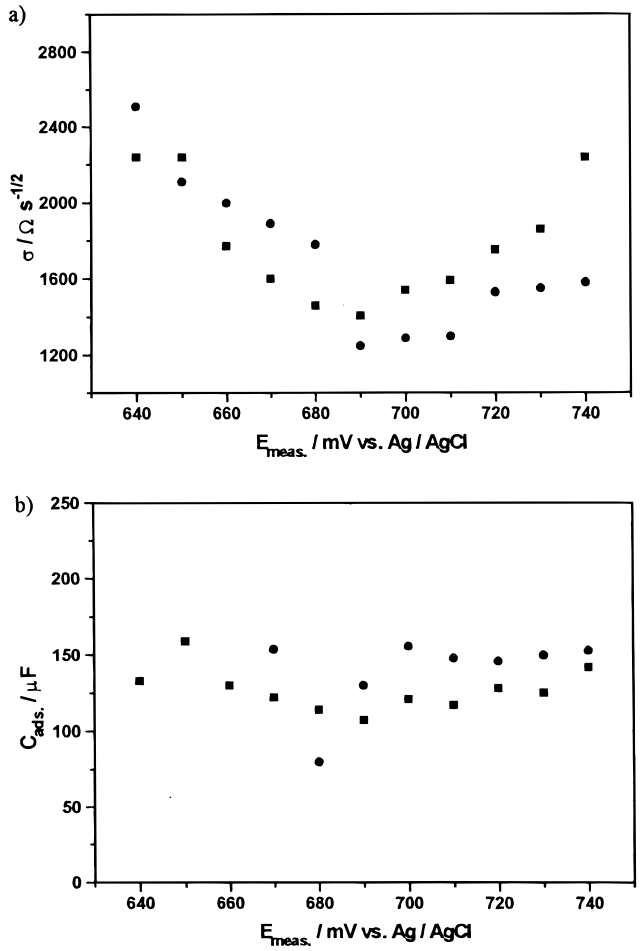

Figure 12. (a) Plot of σ versus the electrode potential for the Cu2.5-un (●) and the Cu2.5-ox (■) composite electrodes. (b) Plot of C_{ads} versus the electrode potential for the Cu2.5-un (●) and the Cu2.5-ox (■) composite electrodes.

conduction band. Interestingly, the diffusion coefficients of electrons in p-type silicon semiconductors range from 2 to 40 $cm^2\ s^{-1}$.[33] The specific resistance of 82 Ω cm is a value typical for semiconducting materials.

The charge-transfer resistance $R_{ct,2}$, describing the transfer of K^+ between the electrolyte solution and the solid Cu hcf, is also independent of the oxidation of the graphite. This can easily be rationalized because this charge transfer occurs at the interface between the Cu hcf and the electrolyte solution. A plot of $R_{ct,2}$ versus electrode potential exhibits a minimum at the formal potential of the hexacyanoferrate system of the solid Cu hcf (see Figure 11a). To understand this, one has to assume that in this frequency range an electron hopping mechanism is operative together with the cation diffusion. In this range, where only a coupled cation and electron transport is possible, the charge-transfer resistance of the potassium ions has therefore also to be dependent on the redox composition of the Cu hcf, thereby maintaining the charge-transfer rate constant at $(3.0 \pm 0.2) \times 10^{-6}$ m s^{-1} (see Table 1). This constancy of the charge-transfer rate is an additional indication for the correctness of the assumption of a coupled cation−electron transport as well as the electron hopping. The minimum in the potential dependence of the charge-transfer resistance can be explained with the following equation[34,35]

$$R_{ct,2} = \frac{RT}{n^2F^2A(c_{ox}^0)^{\alpha}(c_{red}^0)^{\beta}k_s} \tag{10}$$

where k_s is the standard rate constant and $c_{ox}{}^0$ and $c_{red}{}^0$ are the concentrations of oxidized and reduced centers in the solid compound.

The product $c_{ox}{}^0$ and $c_{red}{}^0$ has a maximum value when the ratio c_{ox}/c_{red} becomes one. This is the situation at the formal potential of copper hexacyanoferrate. $C_{dl,2}$ is the double layer capacity associated with the charge transfer of K^+. It is also independent of the type of graphite used and the applied potential (see Figure 11b). The value of $C_{dl,2}$ is (0.41 ± 0.08) mF cm^{-2}. An insertion reaction of ions into solid materials can be controlled by diffusion of the ions. The corresponding Warburg coefficient σ[36] is the same for both electrodes (see Figure 12a). This is understandable because the diffusion of K^+ ions also takes place inside the Cu hcf and not at the graphite surface. The Warburg coefficient shows a minimum at the formal potential of copper hexacyanoferrate (690 mV) which is fully in line with the proposed coupled cation−electron transport depending on the redox composition of the Cu hcf. This is expressed in the following equation:[27]

$$\sigma = \frac{V_M|dE/dy|}{zFA(2D)^{1/2}} \tag{11}$$

V_M and y are defined as the molar volume of the electroactive species and the molar fraction of the mobile potassium ions in the net reaction according to eq 1, respectively.

Thus, the Warburg coefficient will have a minimum according to the following derivation

$$E - E_f = \frac{RT}{2zF}\ln\frac{a_{ox}}{a_{red}} \tag{12}$$

E_f is the formal potential of the hexacyanoferrate system in the solid

$$E - E_f = \frac{RT}{2zF}\ln\frac{1-y}{y} \tag{13}$$

$$\left|\frac{dE}{dy}\right| = \frac{RT}{2zF}\frac{1}{y(1-y)} \tag{14}$$

$|dE|/|dy|$ has a minimal value for $y = {}^1/_2$, which means for $E = E_f$. For $y \rightarrow 0$ or $y \rightarrow 1$ it follows that $|dE|/|dy| \rightarrow \infty$. Minima in the Warburg coefficient have also been found by Armstrong et al.[37] for graphite electrodes covered by poly(4-vinylpyridine) films containing $IrCl_6^{2-}/IrCl_6^{3-}$ species. This allows the diffusion coefficient of potassium ions in copper hexacyanoferrate to be determined. The numerical value $(1.4 \pm 0.2) \times 10^{-9}$ $cm^2\ s^{-1}$ can be obtained from the Warburg coefficient according to the following equation:

$$D = \frac{V_M^2\left(\frac{RT}{zF}\left|\frac{1}{y(1-y)}\right|\right)^2}{z^2F^2A^2 2\sigma^2} \tag{15}$$

It is certainly a nice indication of the correctness of this value that practically the same has been found by cyclic voltammetry (see Table 1).

The adsorption capacity is independent of the type of graphite and also independent of the applied potential. Its relatively large value of (53 ± 2) mF cm^{-2} (see Figure 12b) is probably due to the fact that the charged ions are adsorbed at the rough surface of the Cu hcf.

Conclusions

This study was aimed at improving the understanding of the complex reaction mechanisms of redox processes in solid copper hexacyanoferrate incorporated in composite electrodes and mechanically attached to a graphite electrode surface. The experimental results from cyclic voltammetry, chronocoulometry and electrochemical impedance spectroscopy allowed to build up a detailed and self-consistent model of the elementary processes associated with the oxidation and reduction of the low-spin iron ions in solid Cu hcf. For the first time, a careful simulation of the impedance data on the basis of different models allowed the separation of the diffusion of cations (K^+) and of electrons. The diffusion coefficient obtained for the electron transport obviously results from the semiconductor properties of the Cu hcf. The electron hopping between the redox centers, which can be formulated as an electron exchange reaction

$$\{Fe^{*3+}-CN-Cu-NC-Fe^{2+}\} \leftrightarrow \{Fe^{*2+}-CN-Cu-NC-Fe^{3+}\}$$

proceeds with a rate k. This k must be either so small that this way of electron propagation is frozen in the MHz range, or it cannot operate at these frequencies because it is only sustained with a "local charge compensating" diffusion of cations. Conduction of electrons in the conduction band does not need this local charge compensation as the band structure is per se a delocalized structure. The final conclusion of this study is that again a separation of cation diffusion and electron hopping has not been achieved, probably because these two processes are so interdependent that a separate measurement of their rates is impossible. The diffusion controlled insertion of potassium cations obeys the Randles mechanism. The electron transport through the solid toward the reaction zone occurs via the conduction band of the semiconducting solid, whereas the electron transport within the reaction zone may be described as electron hopping between the redox centers coupled with the transport of the charge compensating potassium ions.

Acknowledgment. We acknowledge the support by Deutsche Forschungsgemeinschaft and Fonds der Chemischen Industrie.

References and Notes

(1) Düssel, H.; Komorsky-Lovrić, Š.; Scholz, F. *Electroanalysis* **1995**, *7*, 889.
(2) Kahlert, H.; Dostal, A.; Scholz, F. *Fresenius' J. Anal. Chem.* **1996**, *355*, 21.
(3) Kahlert, H.; Komorsky-Lovrić, Š.; Hermes, M.; Scholz, F. *Fresenius' J. Anal. Chem.* **1996**, *356*, 204.
(4) Kahlert, H.; Scholz, F. *Electroanalysis* **1997**, *9*, 922.
(5) Engel, D.; Grabner, E. W. *Ber. Bunsen-Ges. Phys. Chem* **1985**, *89*, 982.
(6) Siperko, L. M.; Kuwana, T. *J. Electrochem. Soc.* **1983**, *130*, 396.
(7) Amos, L. J.; Duggal, A.; Mirsky, E. J.; Ragonesi, P.; Bocarsly, A. B.; Fitzgerald-Bocarsly, P. A. *Anal. Chem.* **1988**, *60*, 245.
(8) Moon, S. B.; Xidis, A.; Neff, V. D. *J. Phys. Chem.* **1993**, *97*, 1634.
(9) Schneemeyer, L. F.; Spengler, S. E.; Murphy, D. W. *Inorg. Chem.* **1985**, *24*, 3044.
(10) Gao, Z.; Bobacka, J.; Ivaska, A. *Electrochim. Acta* **1993**, *38*, 379.
(11) Engel, D. Ph-D Thesis, Frankfurt, 1988.
(12) Siperko, L. M.; Kuwana, T. *Electrochim. Acta* **1987**, *32*, 765.
(13) Feldman, B. J.; Murray, R. W. *Anal. Chem.* **1986**, *58*, 2847.
(14) Feldman, B. J.; Feldberg, S. W.; Murray, R. W. *J. Phys. Chem.* **1987**, *91*, 6558.
(15) Feldman, B. J.; Murray, R. W. *Inorg. Chem.* **1987**, *26*, 1702.
(16) Kinoshita, K. *Carbon, Electrochemical and Physicochemical Properties*; Wiley: New York, 1988.
(17) Mamatow, G.; Freeman, D. B.; Miller, F. J.; Zittel H. E. *J. Electroanal. Chem.* **1965**, *9*, 305.
(18) Blurton, K. F.; Greenberg, P.; Oswin, H. G.; Rutt, D. R. *J. Electrochem. Soc.* **1972**, *119*, 559.
(19) Evans, J. F.; Kuwana, T.; Henne, M. T.; Royer, G. P. *J. Electroanal. Chem.* **1977**, *80*, 409.
(20) Gomathi, H.; Prabhakara Rao, G. *J. Electroanal. Chem.* **1985**, *190*, 85.
(21) Clem, R. G. *Anal. Chem.* **1975**, *47*, 1778.
(22) Kamau, G. N.; Willis, W. S.; Rusling, J. F. *Anal. Chem.* **1985**, *57*, 545.
(23) Cabanis, G. E.; Diamantis, A. A.; Rorer Murphy Jr., W.; Linton, R. W.; Meyer, T. J. *J. Am. Chem. Soc.* **1985**, *107*, 1845.
(24) Scholz, F.; Lange, B. *Trends Anal. Chem.* **1992**, *11*, 359.
(25) Scholz, F.; Meyer, B. *Voltammetry of solid Microparticles Immobilized on Electrodes Surfaces* in *Electroanal. Chem.*; Bard, A., Rubinstein, I., Eds.; Marcel Dekker: New York, 1998; Vol. 20, p 1.
(26) Nicholson, R. S. *Anal. Chem.* **1965**, *37*, 1351.
(27) Macdonald, J. R. *Impedance Spectroscopy*; John Wiley & Sons: New York, 1987.
(28) Buck, R. P. *J. Electroanal. Chem.* **1986**, *210*, 1.
(29) Albery, W. J.; Elliott, C. M.; Mount, A. R. *J. Electroanal. Chem.* **1990**, *288*, 15.
(30) Drossbach, P.; Schulz, J. *Electrochim. Acta* **1964**, *9*, 1391.
(31) Lovrić, M.; Scholz, F. *J. Solid State Electrochem.* **1997**, *1*, 108.
(32) Xidis, A. Neff; V. D. *J. Electrochem. Soc.* **1991**, *138*, 3637.
(33) Wolf, H. *Silicon Semiconductor Data*, Pergamon Press: Oxford, 1969; p 92.
(34) Galus, Z. *Fundamentals of Electrochemical Analysis*, 2nd ed.; Ellis Horwood: New York, 1994; p 257.
(35) Sluyters-Rehbach, M.; Sluyters, J. H. *Electroanal. Chem.* **1970**, *4*, 1−128.
(36) Ho, C.; Raistrick, I.; Huggins, R. *J. Electrochem. Soc.* **1980**, *127*, 343.
(37) Armstrong, R. D.; Lindholm, B.; Sharp, M.; *J. Electroanal. Chem.* **1986**, *202*, 69.